Received: 29 May 2023 | Revised: 9 July 2023 | Accepted: 27 July 2023

DOI: 10.1111/tra.12915

RESEARCH ARTICLE

Traffic WILEY

Combination of hydrophobicity and codon usage bias determines sorting of model K^+ channel protein to either mitochondria or endoplasmic reticulum

Anja J. Engel[1] | Steffen Paech[2] | Markus Langhans[2] | James L. van Etten[3] | Anna Moroni[4] | Gerhard Thiel[1] | Oliver Rauh[1]

[1]Faculty of Biology, Technical University of Darmstadt, Darmstadt, Germany

[2]Faculty of Chemistry, Macromolecular and Paper Chemistry, Technical University of Darmstadt, Darmstadt, Germany

[3]Department of Plant Pathology and Nebraska Center for Virology, University of Nebraska-Lincoln, Lincoln, Nebraska, USA

[4]Department of Biosciences and CNR IBF-Mi, Università degli Studi di Milano, Milan, Italy

Correspondence
Oliver Rauh, Faculty of Biology, Membrane Biophysics, Technical University of Darmstadt, Schnittspahnstrasse 3, 64287 Darmstadt, Germany.
Email: rauh@bio.tu-darmstadt.de

Funding information
DFG Priority Program, Grant/Award Number: SPP1926; European Research Council (ERC), Grant/Award Number: 695078; Fondazioner Telethon Grant, Grant/Award Number: GGP20021

Abstract

When the K^+ channel-like protein Kesv from *Ectocarpus siliculosus virus* 1 is heterologously expressed in mammalian cells, it is sorted to the mitochondria. This targeting can be redirected to the endoplasmic reticulum (ER) by altering the codon usage in distinct regions of the gene or by inserting a triplet of hydrophobic amino acids (AAs) into the protein's C-terminal transmembrane domain (ct-TMD). Systematic variations in the flavor of the inserted AAs and/or its codon usage show that a positive charge in the inserted AA triplet alone serves as strong signal for mitochondria sorting. In cases of neutral AA triplets, mitochondria sorting are favored by a combination of hydrophilic AAs and rarely used codons; sorting to the ER exhibits the inverse dependency. This propensity for ER sorting is particularly high when a common codon follows a rarer one in the AA triplet; mitochondria sorting in contrast is supported by codon uniformity. Since parameters like positive charge, hydrophobic AAs, and common codons are known to facilitate elongation of nascent proteins in the ribosome the data suggest a mechanism in which local changes in elongation velocity and co-translational folding in the ct-TMD influence intracellular protein sorting.

KEYWORDS
codon usage, effect of synonymous codon exchange, membrane protein sorting, transmembrane domain hydrophobicity

1 | INTRODUCTION

Eukaryotic cells have developed efficient systems for targeting nascent membrane proteins to their final destinations in either the plasma membrane or membranes of intracellular organelles like mitochondria or chloroplasts.[1] While most proteins are exclusively sorted to one target membrane, some proteins also exhibit dual targeting, meaning that the same or a similar variant is functional in the plasma membrane and in an organelle membrane.[2,3]

Typically, synthesis of membrane proteins begins in the cytosol, regardless of the final target destination. The canonical pathway for most plasma membrane proteins involves specific motifs at the N-terminus of the nascent polypeptide that interact with the signal recognition particle (SRP).[1] This complex guides the ribosome together with the nascent polypeptide to the translocon in the endoplasmic reticulum (ER), which serves as the entry point for further

Anja J. Engel and Steffen Paech should be considered joint first authors.

protein synthesis.[4] In addition to this canonical pathway, there are other SRP-independent routes for targeting membrane proteins in the ER. One well-known alternative involves tail-anchored (TA) proteins.[5] In this case, a transmembrane domain (TMD) at or near their C-termini is recognized by a complex of chaperones at the exit tunnel of the ribosome. The so-called guided entry of tail-anchored proteins (GET) complex in yeast or the transmembrane recognition complex (TRC) in humans further ushers the nascent protein to the ER membrane for insertion.[6–8] Recently an additional SRP-independent (SND) pathway for ER sorting was identified not only in yeast,[9] but also in mammalian cells.[10] In this pathway, client proteins are eventually inserted into the ER after binding to SND proteins in the central region of their TMDs.

In contrast, membrane proteins destined for mitochondria or chloroplasts avoid these targeting systems. After synthesis, they are guided by chaperones to the mitochondrial or chloroplast translocation apparatus and inserted in a post-translational manner into their target membranes.[11] However, it is still only poorly understood how these proteins are targeted to the organelle import sites.[1]

While co-translational protein synthesis into the ER and post-translational synthesis of organelle proteins were traditionally seen as two independent processes, recent data indicate a mutual interplay between the ER and mitochondria/chloroplasts, in particular in the context of protein biogenesis of organelle proteins.[1] In a so-called ER-SURF mechanism, the surface of the ER and its associated chaperons operate as a sorting hub. They provide the pathway for co-translational synthesis of proteins for the secretory pathway but serve also as a distribution hub for proteins, which are eventually targeted to the mitochondria.[1]

An interesting experimental system for obtaining more unbiased information on the mechanisms, which determine the sorting of membrane proteins in mammalian cells, is provided by viral proteins. It is well known that viruses hijack the cellular machinery for transcription, translation and protein targeting and make use of these pathways for their own purposes. Analysis of these viral pathways has in this way helped to uncover basic cellular mechanisms, which would have been otherwise difficult to study.[12,13] A promising system for studying intracellular sorting of membrane proteins in cells is provided by K^+ channel proteins from dsDNA viruses, which infect eukaryotic algae.[14] The viral coded proteins have a monomer size of only around 100 amino acids, truly minimal, but still contain all the structural hallmarks of eukaryotic K^+ channels. With these features, the viral proteins are ideal orthogonal model systems to examine basic cell biological processes in eukaryotic cells.[15] A seminal observation, which makes these proteins so interesting as a model system for protein sorting, is that one channels, Kcv, is in mammalian cells co-translationally synthesized at the translocon into the ER,[16] from where it travels via the secretory pathway to the plasma membrane.[17] In contrast the structurally similar Kesv protein is sorted post-translationally to the inner membrane of the mitochondria[18] via the canonical TIM/TOM translocases.[19] Studies with yeast have shown that a decision between the two sorting pathways occurs at the translational stage of the nascent proteins on the ribosome and is decided by their affinity for the SRP.[20] While the Kcv channel binds the SRP, Kesv does not.

A series of studies have shown that sorting of the Kesv channel to the mitochondria can be redirected by two distinct manipulations, namely insertion of amino acids (AAs) into the C-terminal TMD[19–21] and by manipulation of codon usage.[22] In the first case, it was observed that insertion of two or three valines into the C-terminal TMD (ct-TMD) of this channel redirected protein sorting from the mitochondria to the secretory pathway.[19,20] This insertion of additional amino acids elongated the ct-TMD of Kesv to the length of the ct-TMD in the Kcv channel.[19] Figure 1B shows a structural model of the N- and C-terminal transmembrane domains (nt-TMD and ct-TMD) for a Kesv monomer, with and without insertion of three valines in position 113. The reason for a rerouting of sorting after insertion of valines in this position is that the Kesv protein becomes a substrate for the GET sorting pathway in yeast.[20]

Subsequent mutational studies in the Kesv ct-TMD were not compatible with the idea that the length of this domain is responsible for sorting.[21] Also, these studies did not identify an obvious amino acid motive in the ct-TMD that might serve as a binding motive for a chaperon.[21] From the results of these experiments, it was suggested that alternative factors might be relevant for the sorting of these proteins. In a recent study, it was found the codon choice could be such a sorting factor because Kesv targeting to the mitochondria was substantially altered by manipulation of the codon choice.[22] Sorting of Kesv to the mitochondria was augmented when the channel was expressed from a synthetic gene in which rare codons were exchanged for codons which are common in mammalian cells. Chimeras with rare and common codons generated an even more complex sorting pattern, in that they were able to redirect sorting of Kesv into the ER. In some chimeras, the protein could even be seen in the same cells in both ER and

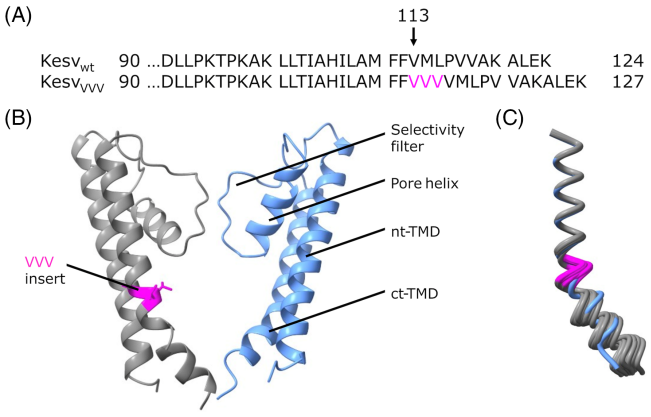

FIGURE 1 Predicted structure of Kesv with and without insertion of valines in the C-terminal transmembrane domain. (A) Primary sequence of ct-TMD from wt Kesv and with insertion of AAs triplet VVV in position 113 (Kesv$_{+VVV}$). (B) Pore domain Kesv protein with labeling of structural elements. The image depicts only two of the four monomers without the cytosolic C terminal domain (AA 1–32). A wt monomer is shown in blue (right) and a mutant monomer with an insertion of three Valines (Kesv$_{+VVV}$) in grey (left). The three valines in position 113 are highlighted in magenta. (C) Overlay of ct-TMD (AAs 87-c-Term) with all three AA inserts listed in Table S1. Wt in blue, mutants in grey, inserted AAs in magenta.

mitochondria.[22] Collectively, the data suggest that codon usage bias (CUB) in a gene in combination with cellular factors can serve as a secondary code for sorting of membrane proteins.

Here, we take advantage of the sensitivity of Kesv sorting to changes in the AA composition in the ct-TMD and to codon choice in order to examine the impact of these parameters on intracellular protein trafficking. To this end, we systematically varied the triplet of AAs, which was inserted into the ct-TMD of Kesv, and monitored the impact of these manipulations on sorting as a function of AA flavor and codon choice. The data show that the intracellular targeting of Kesv depends on both the physicochemical character of the AA triplet as well as on CUB. Sorting to the mitochondria is strongly imposed by a cationic AA in this region of the protein. Targeting to the same destiny is also augmented by a combination of hydrophilic AAs and CUB with the effect that rare codons and hydrophilic AAs favor sorting to the ER while the combination of hydrophobic AAs and common codons shift sorting to the mitochondria.

2 | RESULTS AND DISCUSSION

2.1 | Insertion of AA triplet in C-terminal transmembrane domain affects Kesv sorting in AAs and position-dependent manner

In previous studies, the Kesv protein was no longer sorted to the mitochondria but to the ER after insertion of a pair or triplet of valines into position 113 in the ct-TMD.[19–21] To better understand the dependency of this shift in sorting on the flavor of the inserted AAs, we prepared 14 additional constructs with randomly chosen AA triplets ($Kesv_{+3}$). These constructs and the wt protein were expressed with a C-terminal eGFP-tag in HEK293 cells and their cellular localization was examined 16 h after transfection. The sorting destiny of the constructs was evaluated according to the distribution of the eGFP-tag in cells (for details, see Section 4).

Like in a previous study,[22] we found that the wt protein was targeted in >60% of the cells into the mitochondria (Figure 2A). In a small fraction of cells, the protein could also be identified in the ER (2%; Figure S1A). In the remaining cells, the GFP fluorescence was distributed throughout the cell, including the nucleus (Figure 2A). We interpret the latter phenotype, which is characterized by low fluorescence signal in either ER and mitochondria and an equally strong GFP signal in cytosol and nucleus, as unsorted and or degraded.[22] The GFP tag is presumably cleaved from the degraded protein, with the effect that it can enter the nucleus. Since the images provide no detailed information on the destination, integrity, and fold of the protein, we classify this phenotype as unsorted/degraded.

Insertion of a randomly chosen AA triplet into the TMD of Kesv had construct-specific impacts on sorting. The results of intracellular sorting in Figures 2A and S1A can be divided into three different phenotypes. In the first category (type I) the protein is no longer seen in the ER. With the insertion of the AA triplet SKA ($Kesv_{+SKA}$) and VTK ($Kesv_{+VTK}$) the protein is exclusively found in the mitochondria (Figure 2A,B); $Kesv_{+PSV}$ is also detected in this organelle but appears frequently as unsorted/degraded (Figure 2A). In the type II case, the

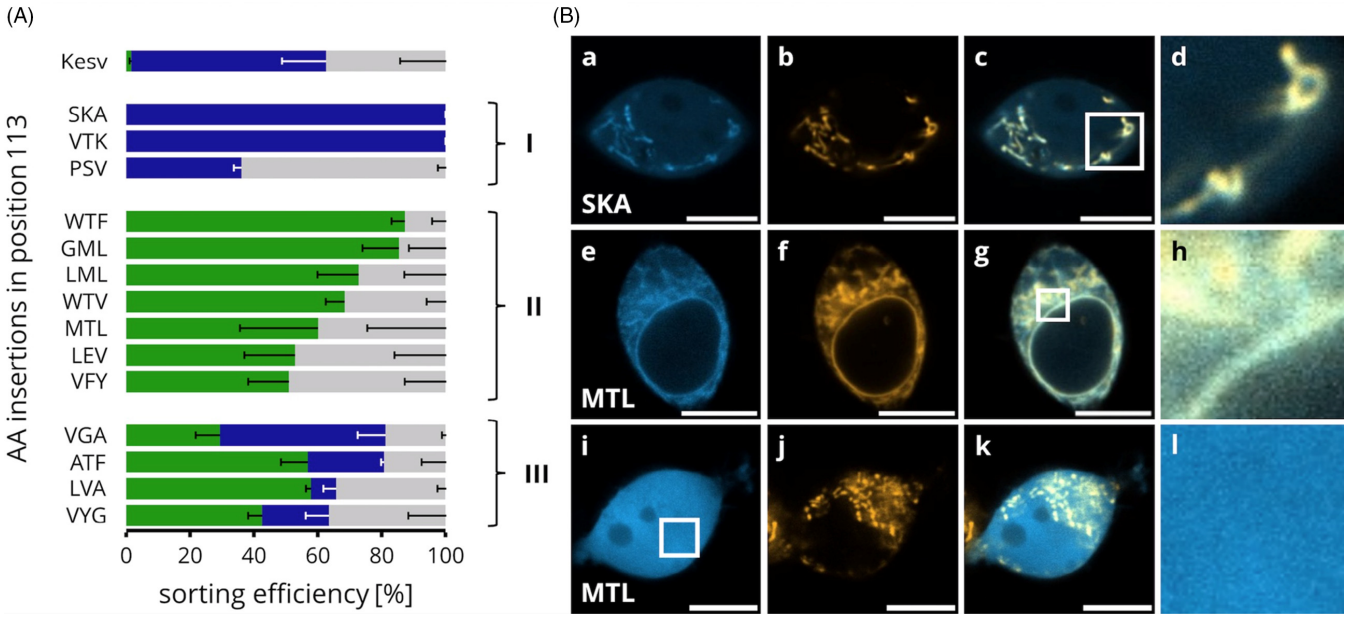

FIGURE 2 Sorting destiny of Kesv wt and Kesv with insertion of AA triplets in ct-TMD. (A) Mean relative distribution of Kesv wt and Kesv constructs with insertion of indicated triplets of AAs ($Kesv_{+3}$) in position 113 of the ct-TMD. Sorting to mitochondria (blue), ER (green) or unsorted/degraded (grey) is classified into three categories: type I, sorted to mitochondria and un-sorted; type II, ER and un-sorted; type III, ER or mitochondria or unsorted/degraded. Each column is a mean value ± SD of N ≥ 3 independent experiments with a total of ≥150 cells per column. (B) Exemplary fluorescent images of HEK293 cells transfected with $Kesv_{+3}$ constructs. a, e and i: eGFP-tagged $Kesv_{+3}$ constructs; b and j: MitoTracker™ Red, f: ER-Tracker™ Red; c, g and k: Overlay images of the two channels in the same row; Scale bars in B-L 10 µm. d, h and l: Enlarged details in white frames.

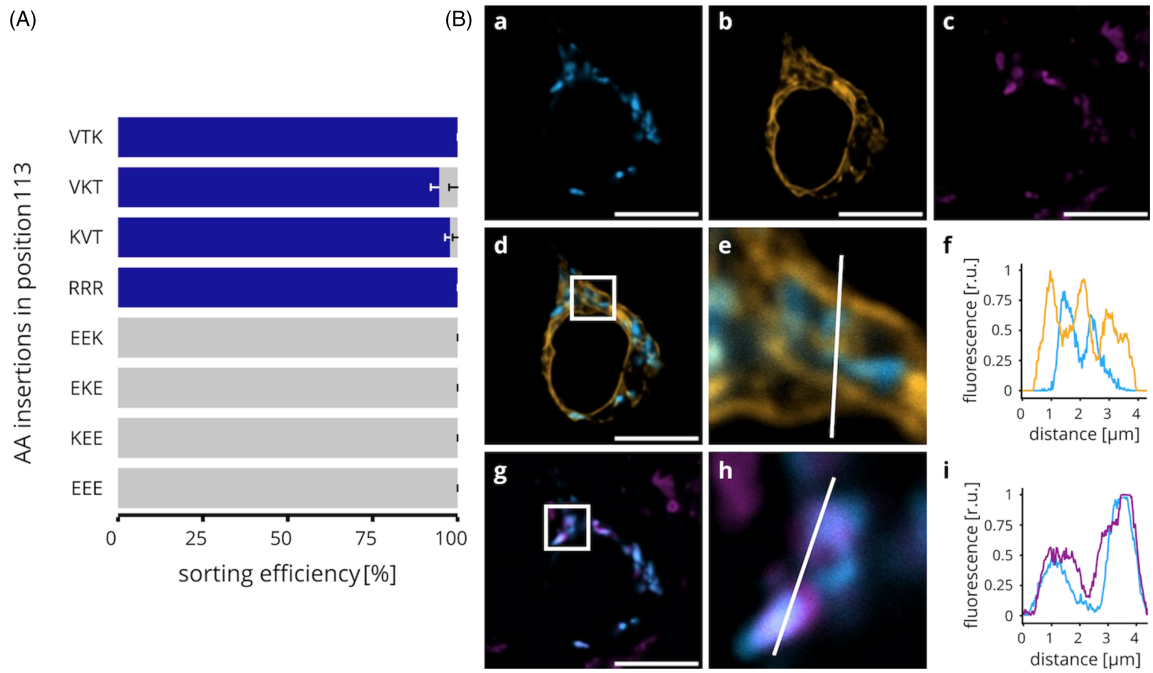

FIGURE 3 Sorting of Kesv$_{+3}$ constructs including AAs with charged side chain. (A) Mean relative distribution for localization of Kesv constructs with insertion of triplets of AA (Kesv$_{+3}$) containing a charged AA in position 113 of ct-TMD. Constructs were sorted to mitochondria (blue), or unsorted/degraded (grey). Each column is a mean value ± SD of $N \geq 6$ independent experiments with a total of ≥300 cells per column. (B) Fluorescent images of an exemplary HEK293 cell transfected with Kesv$_{+VTK}$. (a) Kesv$_{+VTK}$::eGFP; (b) ER marker HDEL::mCherry, (c) MitoTracker™ DeepRed; (d and e) Overlay images of the two channels in the same row; (g and h) Enlarged image details as indicated by the white frames; (f and i) Normalized fluorescence intensity along the lines indicated in (d) and (g), respectively. Maxima in the GFP signal (blue) in (f) coincide with minima in the ER marker signal (yellow). In (i), the GFP signal colocalizes with the signal of MitoTracker™ (red). Scale bars a–d, g: 16 µm.

protein is either sorted to the ER or unsorted/degraded. In particular, two constructs, namely Kesv$_{+GML}$ and Kesv$_{+WTF}$, exhibited a very robust sorting to the ER; they were both detected in ≥85% of the cells in this organelle (Figures 2A and S1A). In the remaining five constructs, the frequency of detecting the protein in the ER decreased, while the propensity for unsorting increased. Images in Figure 2B show two examples for Kesv$_{+MTL}$ in which the protein is well sorted to the ER in one cell and unsorted/degraded in the second cell.

The constructs of the type III phenotype exhibited a mixed sorting in that the protein appeared in a construct-dependent manner with different propensities either in the mitochondria or the ER. In the same experiments, the protein was detected either in the mitochondria or in the ER of individual cells (Figures 2A and S1A). The results of these experiments are in good agreement with the conclusion drawn from previous studies, in that the same sorting signal in the Kesv protein can be interpreted by two individual cells in a different manner.[22]

2.2 | Cationic AAs impose mitochondrial sorting

We first addressed the question of whether cationic AAs in the VTK and SKA triplets serve as a strong signal for mitochondrial sorting. We constructed mutants with three Arg insertions (Kesv$_{+RRR}$) and varied in Kesv$_{+VTK}$ the position of the Lys into KVT and VKT in Kesv$_{+VTK}$. Expression of these mutants resulted in all cases in a robust and near-exclusive sorting of the protein into the mitochondria (Figures 3A,B and S1B). The results of these experiments indicate a strong positive impact of a cationic AA in this region of the transmembrane domain for effective mitochondrial sorting; the precise location of the positive charge does not seem to be important for sorting. To further test the impact of such a local positive charge on sorting, additional constructs were made, which contained a triplet of anionic AAs (Kesv$_{+EEE}$) or a combination of anionic and a cationic AAs (Kesv$_{+EKE}$, Kesv$_{+KEE}$ and Kesv$_{+EEK}$). In all cases, these constructs were neither sorted to the ER nor to the mitochondria (Figures 3A and S1B). Hence, a negative charge suppresses the positive effect of a cationic AA on mitochondrial sorting. An alternative interpretation that an anionic amino acid is in general deleterious for protein folding and causes for this reason a complete unsorted/degraded phenotype, is less likely. Notably, insertion of the LEV triplet still re-directs protein sorting to the ER (Figure 1A).

Together with the results of the sorting of the Kesv$_{+LEV}$ construct (Figure 2A) these data indicate a negative effect of an anionic AA on Kesv$_{+3}$ sorting not only to the mitochondria but to sorting in general.

We next tested if the impact of the triplets in redirecting Kesv$_{+3}$ sorting from the mitochondria to the ER sorting, was site specific. For these experiments, we choose the GML triplet, which together with

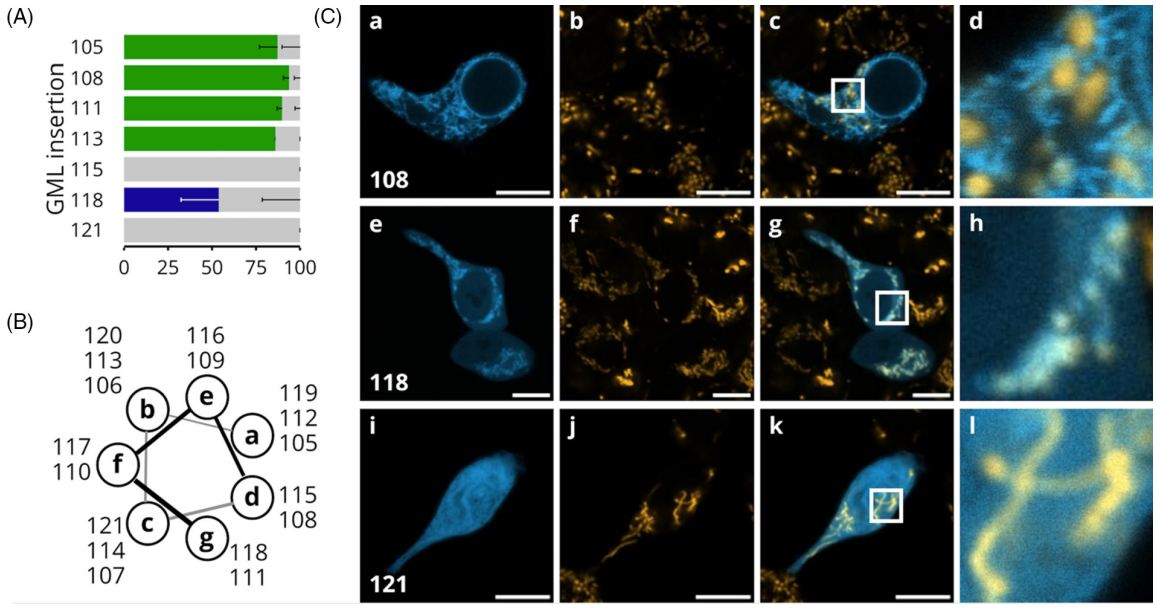

FIGURE 4 Sorting destiny of $Kesv_{+GML}$ inserted between positions 105 and 121. (A) Mean relative distribution for localization of Kesv constructs with insertion of GML triplet in seven different positions between 108 and 121 of ct-TMD. Constructs were sorted to mitochondria (blue), ER (green) or unsorted/degraded (grey). Each column is a mean value (±SD) of $N \geq 3$ independent experiments with a total of ≥150 cells per column. (B) Helix wheel indicating the relative positions for triplet insertion on alpha-helical TMD; (C) Exemplary fluorescent images of HEK293 cells transfected with $Kesv_{+GML}$ in positions 108 (top row), 118 (middle row) and 121 (lower row). (a, e and i): eGFP-tagged $Kesv_{+3}$ constructs; (b, f and j): MitoTracker™ Red; (c, g and k): Overlay images of the two channels in the same row; (d, h and l): Enlarged details in white frames. Scale bars: c–e, g–i, k–m: 10 μm.

the WTL triplet is most effective for shifting the sorting of $Kesv_{+3}$ from the mitochondria to the secretory pathway (Figure 2A). Because of the importance of codon usage for protein sorting, which will be examined later in this study, we favored the GML over the WTV triplet because the former provides more opportunities for using synonymous codons for all three amino acids. To obtain information on the site specificity the GML triplet was inserted in three positions upstream and three positions downstream of the 113 site. Figures 4 and S1C show the quantitative analysis for the sorting of all constructs with GML insertions at different positions in a large number of cells (A) and some characteristic images for the corresponding diversity of sorting of the constructs (Figures 4C and S1C). The results indicate the importance of the position in which the AA triplet is inserted for sorting. While insertion of the GML triplet upstream of position 113 has little influence on protein sorting, the picture is different at the downstream positions. When the triplet is inserted downstream of position 113, $Kesv_{+GML}$ is no longer sorted to the secretory pathway (Figures 4A and S1C). With the GML triplet in positions 115 and 121, the protein appears to be entirely unsorted/degraded. This phenomenon is not necessarily the consequence of failed sorting; for example, it could also arise from the fact that insertion of the triplet in these positions prevents for some other reasons the synthesis of the entire protein. This alternative interpretation of the data does not hold true for the finding that insertion of the GML triplet in position 118 again favors sorting of the protein to the mitochondria with a propensity similar to the wt protein (Figure 4A). These data clearly indicate that the effect of triplet insertion on $Kesv_{+3}$ sorting is site specific.

The data support previous evidence for position dependency of the insertion site for sorting.[19] This dependency does not seem to be related to the helix structure of the transmembrane domain (Figure 4B). Notably, the insertions in positions 108 and 113 are on a helix wheel on the opposite sides but produce the same effect on sorting. In contrast, positions 111 and 118 are on the same side of the helix, but their impact on sorting is very different.

2.3 | Length of C-terminal TMD does not determine sorting

In a previous study, it was speculated that Kesv might be sorted to the mitochondria because of a presumably short ct-TMD. Hence, extension of the ct-TMD by insertion of AAs might serve as a signal for ER sorting.[19] The finding that some of the extensions increase sorting of the Kesv protein to the ER while others do not (Figure 2A), led to a test of this hypothesis. If the length of the ct-TMD is critical for sorting, we expect that AA triplets which favor $Kesv_{+3}$ sorting to the ER, also elongate the transmembrane domain. To test this hypothesis the ct-TMD length and the fold for each construct were predicted with DeepTMHMM,[23] followed by a second prediction of protein folding with AlphaFold.[24] The predicted folds of ct-TMDs with inserted AA triplets are shown in an overlay with the wt Kesv protein in Figure 1C,D. The lengths and folds of all ct-TMD for the different $Kesv_{+3}$ constructs, as they are predicted by DeepTMHMM and measured on the AlphaFold predicted structures in ChimeraX,[25] are also

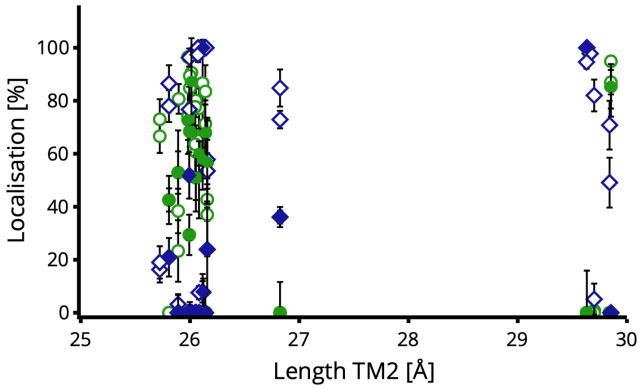

FIGURE 5 Sorting of wt Kesv and Kesv$_{+3}$ constructs as a function of the estimated length of their ct-TMD. After identifying the position of the ct-TMD with DeepTMHMM,[23] for each of the constructs in Figure 2A, the domain fold was predicted with AlphaFold.[24] The length of the respective TMDs was measured as the distance (in Å) between first and last alpha C-atom in this domain with ChimeraX.[25] The propensity for detecting the Kesv$_{+3}$ constructs in the mitochondria (blue) or the ER (green) are plotted as a function of the ct-TMD length.

given in Table S1. These data and the plot in Figure 5 show two distinct populations of ct-TMDs which differ in up to 4 Å in length. But both populations include constructs with a high propensity for sorting to either the mitochondria or the ER (Figure 5). Hence the length of the second TMD is, unlike suggested previously,[19] not important as a sorting signal in the Kesv$_{+3}$ protein.

2.4 | Hydrophobicity of inserted AA triplet influences sorting

Scrutiny of the data in Figure 2 suggests that insertions of hydrophobic AAs promote sorting to the ER while hydrophilic AAs favor trafficking to the mitochondria. To quantify this dependency, the propensity for ER and mitochondria sorting was plotted as a function of the mean hydrophobicity (HyP) of the inserted AA triplets. The latter scale was based on normalized Kyte Doolittle HyP values.[26] Because of the strong impact of charged AAs on sorting (Figure 3), all triplets with a charged AA were excluded from this analysis.

The data from all the remaining triplets show a trend in which the sorting destiny is weakly dependent on AA HyP (Figure 6A). The frequency for sorting of Kesv$_{+3}$ to the ER increased with the HyP of the AA triplet, while sorting to the mitochondria exhibited the inverse trend. The correlation coefficients for both sorting targets support this inverse dependency on HyP. But both values are 0.1257 for sorting to ER and −0.1527 for sorting to mitochondria respectively low and not significant (Figure 6F, $p > 0.05$). The results of these experiments imply that the local HyP of this region of the TMD might be critical for sorting, and that increasing HyP favors sorting to the ER and penalizes sorting to the mitochondria.

2.5 | CUB has an impact on sorting

We had previously reported that sorting of the Kesv protein to mitochondria or ER in mammalian cells can be modulated by the choice of the codons.[22] To estimate the contribution of CUB to the present pattern of Kesv$_{+3}$ sorting, the propensity for trafficking to ER or mitochondria was analyzed as a function of the mean CUB value for the triplet of the inserted amino acids. The CUB value is a human cell-specific measure, which provides the relative frequency of each codon relative to the abundance of that codon to all other codons encoding the same AA.[27] The results in Figure 6B indicate an apparent dependency between sorting and the codon choice of the inserted amino acid triplet. Trafficking of the protein to the ER is supported by common codons, while sorting to the mitochondria is more favored by rare codons. Like in the case of the relationship between sorting and HyP, the correlation coefficients show already stronger tendency but without being significant for the ER sorting (p_{ER} >0.05, $p_{Mito} = 0.037$).

Based on this dual dependency, we asked the question if the sorting destiny of Kesv might be affected by a combination of both factors. Because HyP and rare/varying codons favor sorting to the ER, we plotted the sorting destiny of the Kesv$_{+3}$ constructs as a function of the product of HyP and CUB (HyP × CUB). The data in Figure 6C,F show that consideration of both factors greatly improved the correlation coefficient from 0.1257 to 0.5459 and from −0.1527 to −0.7432 for sorting to the ER and the mitochondria respectively. The latter correlations have a $p_{Mito} = 0.0088$, showing a further increase of significance over CUB alone. However, ER sorting still showed a $p_{ER} > 0.05$.

To address the question if this increase in correlation coefficient is a coincidence, we randomized the CUB values before multiplication with the HyP values and calculated the corresponding correlation coefficient for sorting to the ER. The results of all 39 916 800 possible permutations (Figure S2) show that a correlation coefficient of >0.5459 occurs in only 1.36% of all possible combinations. The result of this analysis strongly supports the conclusion from Figure 6C that sorting of the Kesv protein is sensitive to a combination of HyP and codon choice at a critical position in the ct-TMD.

To further test the predicted dependency of sorting on codon choice, the Kesv$_{+3}$ constructs from Figure 6A,B were rebuilt by using either the most common (Cmn) or most rare (Rare) codons for the inserted AA triplet. To evaluate the impact of codon choice on sorting, the respective constructs were again expressed with an eGFP-tag in HEK293 cells and examined for their intracellular sorting. The data show that a change in codon choice has for some constructs an appreciable impact on sorting. For example, the Kesv$_{+WTV}$ construct is sorted in 68 ± 6% of the cells to the ER when the choice of codons is random but in 84 ± 4% when the most common codons are used. A compilation of all data shows that a general homogenization of the CUB for either frequent or non-frequent codons increases the correlation between HyP and protein sorting (Figure 6F). This supports the assumption that codon choice plays a role in Kesv sorting. Furthermore, the correlation coefficient is greatly increased when plotting the sorting results of both constructs with the most common and least common codons as a function of HyP × CUB (Figure 6D, E). The

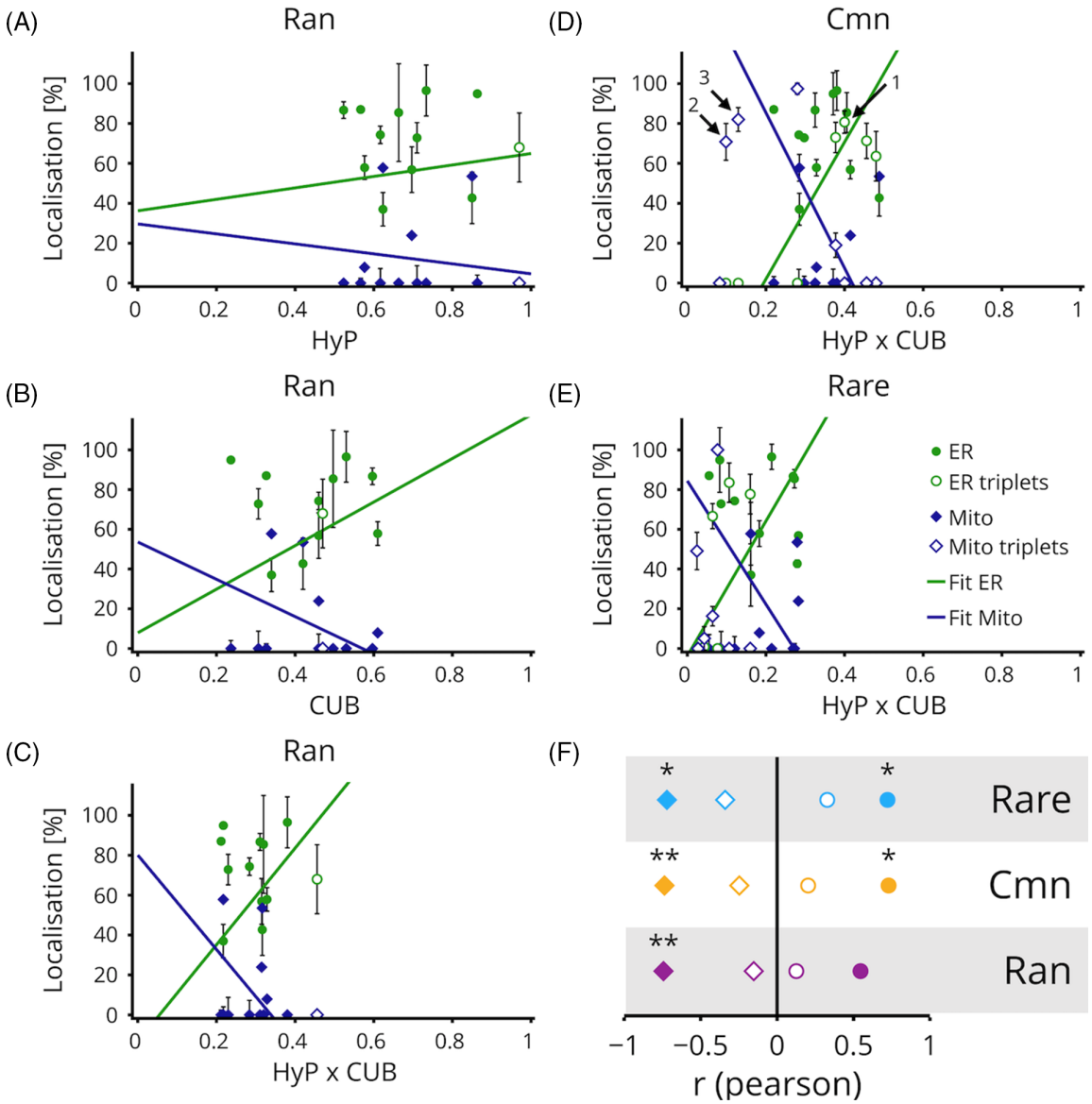

FIGURE 6 The frequency of detecting $Kesv_{+3}$ constructs in the ER or mitochondria. The localization of the $Kesv_{+3}$ constructs from Figure 2 (without charged AA) with a random choice of codons for the inserted AA triplet in the ER (green) or in the mitochondria (blue) as a function of the mean hydrophobicity (HyP) of the AA triplet (A), as a function of the mean codon usage bias (CUB) (B) and as a function of the product of CUB and HyP (C). Localization of the same constructs (filled symbols) plus constructs with triple insertions of the same AA (open symbols) as in C after using most common (D) or least common codons (E) of inserted AA triplet. Filled data points are fitted with Pearson correlation coefficient for ER (green line) and mitochondria (blue line). (F) Mean Pearson correlation coefficients [*r* (Pearson)] for $Kesv_{+3}$ sorting to ER (positive values) or to mitochondria (negative values) from analyzing sorting as function of mean HyP (open symbols) or as a function of the product of HyP and CUB (HyP × CUB, filled symbols) for constructs with randomly chosen codons (Ran, purple), with most common (Cmn, yellow) and least common (Rare, light blue) codons. Each data point in panels A–E is the mean ± SD of three or, in case of the triplets with most common and least common codons, six independent experiments with a total number of 150 or 300 cells respectively for each data point. Arrows in D indicate sorting of $Kesv_{+WWW}$ (1) $Kesv_{+SSS}$ (2) and $Kesv_{+TTT}$ (3). Value of *p* of statistical significance in (F) $^{*}p < 0.05$; $^{**}p < 0.01$.

correlation coefficient becomes significant for constructs with common ($p_{ER} = 0.0108$, $p_{Mito} = 0.0097$) and rare ($p_{ER} = 0.0121$, $p_{Mito} = 0.0124$) codons (Figure 6F).

The present analysis suggests that $Kesv_{+3}$ sorting is critically dependent on a local combination of HyP and codon choice. For a test of this hypothesis, seven additional $Kesv_{+3}$ constructs were created with triplets of the same AA in position 113. For this purpose, AAs with particularly high or low HyP in combination with rare or common codons were chosen. One construct contained also a triple Trp, the AA with only a single codon.

Six of the seven tested constructs show the expected dependency on CUB and Hyp (Figure 6D,E, open points). Constructs with a high HyP × CUB value are sorted with the expected high propensity to the ER, while constructs with a low value are preferentially sorted

to the mitochondria. Worth noting is the ER sorting of the Kesv$_{+WWW}$ construct (Figure 6D, arrow 1). If sorting would only be determined by the HyP of the AAs, this construct should behave like the Kesv$_{+SSS}$ or Kesv$_{+TTT}$ constructs because the latter AAs share the same low HyP of Tryptophan. The high CUB value of Trp, which even exceeds the respective value of the constructs Kesv$_{+SSS}$ or Kesv$_{+TTT}$ with common codons, however, promotes sorting of Kesv$_{+WWW}$ to the ER; the respective Kesv$_{+SSS}$ or Kesv$_{+TTT}$ constructs are preferentially sorted to the mitochondria (Figure 6D, Kesv$_{+SSS}$ arrow 2 and Kesv$_{+TTT}$ arrow 3).

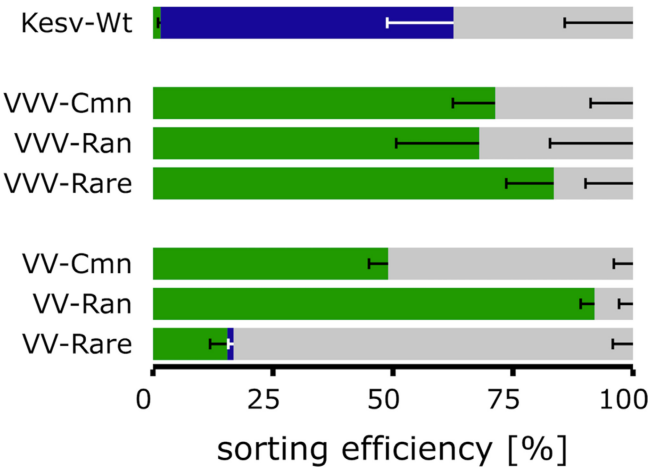

FIGURE 7 Sorting of Kesv wt and Kesv constructs with insertions of two or three Valines in position 113 of ct-TMD. The codons for the two or three Valines were either chosen randomly (ran, comprising common and rare codons), most common (Cmn) or most rare codons (Rare) for expression in human cells. Constructs are sorted to mitochondria (blue), ER (green) or unsorted/degraded (grey). Each column is a mean value ± SD of $N \geq 3$ independent experiments with a total of ≥150 cells per column.

Only the Kesv$_{+QQQ}$ constructs do not fall into this pattern; the triple Q insertion corrupts sorting of the protein to a defined target membrane. An example is shown in Figure S3 for the Kesv$_{+QQQ}$ construct with most common codons. A detailed scrutiny of the image shows that the GFP fluorescence is uniform throughout the cell, including the nucleus. Only regions, which are occupied by either ER or mitochondria, exhibit a low GFP signal. As mentioned before, we interpret this as indirect evidence for a cleavage of GFP from the Kesv$_{+3}$ protein.

Taken together, the data show that protein sorting is depending on a combination of local HyP and CUB. The observations with the Kesv$_{+QQQ}$ construct and with constructs containing a charged AA further indicate that other features of the AA can also influence this sorting procedure.

Previously, it was shown that an insertion of two or three Val in position 113 of Kesv caused a major redirection of this protein from the mitochondria to the ER.[19] Biochemical data with isolated yeast ribosomes had shown that this redirection was related to the fact that the Kesv$_{+VV}$ protein became a target for binding to the GET factor, for example, the chaperone complex which directs tail-anchored proteins into the secretory pathway.[20] Analysis of the Kesv$_{+VVV}$ construct shows that insertion of a valine triplet causes the expected shift of protein sorting, with a strong tendency of trafficking to the ER (Figures 7 and S1C). Direct comparison between the three constructs with different CUB shows that the latter parameter has in this case little effect on sorting of the Kesv$_{+VVV}$ construct (Figure 7). This is different in the Kesv$_{+VV}$ construct. The latter is exclusively sorted to the ER in the case of randomly chosen codons; this effect is abolished by using either common or rare codons for the two positions (Figure 7). Collectively, the results of these experiments suggest, in combination with the aforementioned biochemical data, that the flavor of the inserted AAs determines the binding affinity of Kesv to

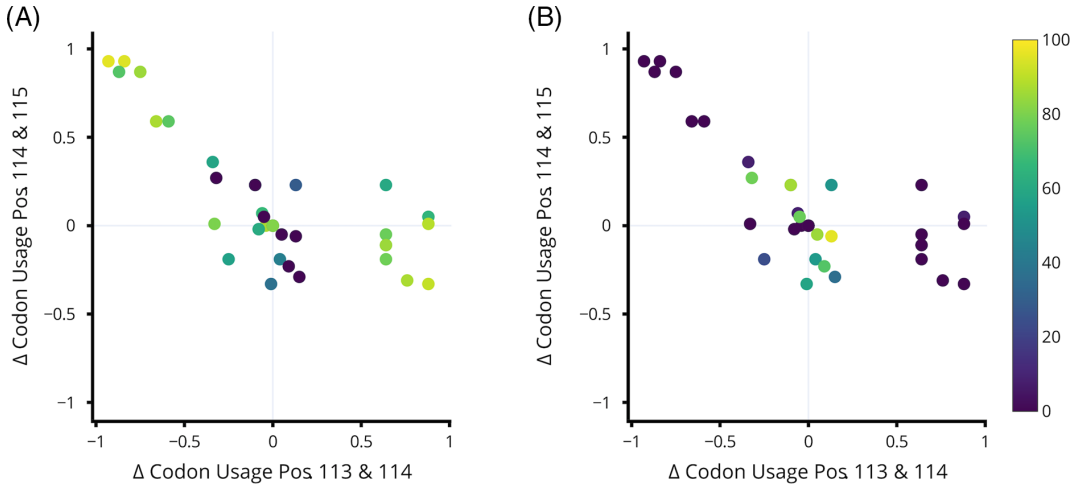

FIGURE 8 Probability for ER or mitochondrial sorting as a function of the step size in CUB within the AA triplet. (A) Probability of finding different Kesv$_{+3}$ constructs from Figure 6 in ER or (B) in mitochondria as a function of codon usage step size between position 113 and 114 (*x*-axis) and step size from position 114 to 115 (*y*-axis). Zero value means that adjacent codons have the same CUB value; negative and positive numbers mean that the codon usage value decreases or increases respectively towards the C-terminus. The probability of a given construct being detected in the ER or mitochondria is color coded between 0% and 100%.

alternative chaperons and that this binding is modulated by CUB of the critical site.

The plot in Figure 8 summarizes the propensity of ER sorting as a function of these step changes in CUB. The data uncover three distinct populations. The propensity for ER sorting is high when CUB is discontinuous, for example, when a common codon in 115 follows a rare codon in position 114 (population 1) and when a common codon in 114 follows an average codon in 113 (population 2). In the case of a uniform CUB for the three AAs, the protein shows a general low propensity for ER sorting (population 3). The same plot for the propensity of mitochondrial sorting shows the inverse relationship. Conditions, like alterations between rare and common codons, which favor ER sorting are dis-favoring mitochondrial sorting. The latter is more supported by a continuity in codons.

3 | CONCLUSIONS

Here, we used a membrane protein with two TMDs, as an orthogonal model system for studying intracellular protein sorting in mammalian cells. Because this protein apparently carries only a weak signal for targeting to the mitochondria, it is possible to reroute its sorting destiny from the mitochondria to the ER by small site-specific modulations in the ct-TMD. The finding that such small and local changes in the TMD of a channel protein could have such drastic impacts on protein sorting suggests that native membrane proteins might be affected in a similar manner not only by mutations, which result in an exchange of amino acids, but even by synonymous mutations.[28] For this reason, the sensitivity of protein sorting to codon usage should also be considered when codons are optimized for example in gene therapy.[28]

Even though the present experimental system is very simple and orthogonal to mammalian cells, we can deduce basic information on the mechanism of membrane protein sorting in mammalian cells. One piece of information is that many $Kesv_{+3}$ constructs show an inverse relationship, in that lowering in the propensity for mitochondria sorting favors targeting to the ER. This suggests that the proteins are presumably synthesized on the same ribosome and that they can in principle be sorted to both destinations; only small changes in the protein favor one sorting route over the other. This concept is supported by the finding that several of the constructs (type III in Figure 2) can be found in the ER of one cell and the mitochondria of another.

The data furthermore uncover a hierarchy of sorting signals which include the flavor of AAs as well as the local CUB. The strongest sorting signal is based entirely on the AAs flavor, with no impact by CUB. One of these signals favoring mitochondrial targeting has at least one cationic AA in the critical region of the ct-TMD. This sorting message is neither sensitive to CUB in the AA triplet nor to its precise position within the triplet. The latter information implies that the mechanism, which affects further sorting steps of the protein, are presumably not binding to a defined AA motive or to a helix fold; they rather seem to sense the general charge in this region of the TMD.

While cationic AAs favor sorting to the mitochondria, anionic AAs suppress this effect. A net negative charge in the critical region not only suppresses targeting to the mitochondria but increases the propensity for complete unsorting of the $Kesv_{+3}$ constructs. Hence, proteins with a net negative charge as well as constructs with a triple Q insertion in this critical position seem to be excluded from the mitochondria. In these cases, the proteins are presumably not binding to any alternative chaperon, with the result that they are degraded. Only cleavage of the GFP from the Kesv protein can explain the images in which the GFP fluorescence is visible in the nucleus but excluded from the ER and the mitochondria.

We previously found that sorting of the same protein could be switched from the mitochondria to the ER either by introducing between 2 and 6 hydrophobic AAs in the ct-TMD[19] or by altering the global or local CUB.[22] The present study confirms that both parameters have an influence on the sorting destiny of the protein and that they operate in a cooperative manner. The sorting destiny of variable $Kesv_{+3}$ constructs can be best described and even predicted by considering the product of local HyP and the CUB of the inserted AA triplet. The data advocate a mechanism in which a combination of hydrophobic AAs and common codons in the critical region of the ct-TMD favor sorting to the ER. The inverse, namely a combination of rare codons and hydrophilic AAs supports targeting to the mitochondria. A more detailed analysis of CUB in the critical domain furthermore indicates that the impact of this parameter is not related to the absolute values of codon frequency but to its relative difference: In the case of a constant CUB, the protein is more frequently sorted to the mitochondria. On the other hand, a sequential order in which a rare codon is following a common codon favors targeting to the ER. This is most evident in the case of the addition of two valines in $Kesv_{+VV}$. From previous experiments, it is known that this insertion of Valines converts the nascent protein into a client for the GET factor on isolated yeast ribosomes.[20] This suggests that a favorable combination of high HyP and CUB in the ct-TMD promotes binding of the GET factor or alternative chaperons to the nascent protein. Interesting in this context is that the best effect for ER sorting is achieved with $Kesv_{+VV}$ in which the codons were chosen randomly (Figure 7). In the latter, the two valines were coded by a sequence of a rare and a common codon, for example, a condition which favors ER sorting according to the data in Figure 7.

The present interpretation of Kesv sorting as a concerted function of HyP and CUB is only based on statistical correlations. Hence, it provides no direct information on the mechanisms, which translates the combination of local HyP and codon usage into different sorting routes of the $Kesv_{+3}$ constructs. While it is well known that HyP of nascent proteins plays a key role in binding and discrimination between different sorting chaperons[29] the role of CUB remains unknown. There is however increasing experimental[30–32] and bioinformatic[33–35] evidence for a distinct role of synonymous codons in fine-tuning the fold of nascent proteins. At this point, it is also important to mention that the CUB value, which was used in this analysis, is only a descriptive

parameter. It only considers if a codon for a particular amino acid is common or rare in the cell type of interest. It does not explicitly account for other crucial parameters like for example the relationship between different codons and the concentration of their corresponding tRNA, stability of the mRNA[36] or the fact that the relative abundances of synonymous codons vary between different amino acids (https://www.genscript.com/tools/codon-frequency-table).

Despite their simplicity, the present data support the hypothesis that rare and common codons affect in some way the velocity of protein synthesis and as a result co-translational folding of the nascent protein.[36–41] In this context, it is interesting to note that a recent study reported that the elongation rate of a nascent protein at the A-site of a ribosome is determined not only by codon usage but also by the charge and HyP of the nascent polypeptide inside the ribosome exit tunnel.[42] Our present findings are fully compatible with these data: A combination of the three parameters, namely positive charge, hydrophobic AAs and frequent codons, which facilitate elongation of the nascent protein,[42] also favor sorting of the $Kesv_{+3}$ protein to the ER. This suggests that the sorting of this protein is sensitive to local changes in the elongation velocity of the nascent polypeptide chain and the resulting dynamics of co-translational folding.

In the context of the mechanisms of protein synthesis, it must be kept in mind that co-translational folding occurs towards the ribosome exit tunnel while the speed of translation is controlled upstream at the A-site of polypeptide elongation. Hence, the codon composition for the inserted AA triplet may not be responsible for the fold of this very AA insert but for the structure downstream of this domain. It is possible that the cooperativity of HyP and CUB of the inserted triplet is not occurring in the same site in Kesv but in different structural elements of the protein. An answer to these questions and more detailed information on the causal relationship between codon usage, protein folding, and protein sorting could be obtained from ribosomal profiling data with various $Kesv_{+3}$ constructs with different degrees of HyP and synonymous codons in the inserted amino acid triplet.

4 | MATERIALS AND METHODS

4.1 | Mutagenesis

Amino acid insertions in the Kesv channel were generated by site-directed mutagenesis as described by DeCero and coworkers[43] using Q5® High-Fidelity 2X Master Mix (New England Biolabs, Ipswich, MA). PCR products were directly used for the transformation of competent *Escherichia coli* XL-1 blue cells by heat shock. Finally, the transformed *E. coli* were plated on LB kanamycin plates and incubated overnight at 37°C.

The colonies were used to inoculate LB medium liquid cultures with 100 µg/mL kanamycin. On the following day, the plasmid DNA was purified using the ZR Plasmid MiniprepTM Classic Kit (Zymo Research; Irvine, CA) and sequenced (Microsynth Seqlab, Göttingen, Germany). Sequencing results were controlled using SnapGene software (GSL Biotech; Chicago, IL).

4.2 | Codon usage adaptation

To create constructs with common codons (Cmn) and rare codons (Rare), a standard human codon frequency table (https://www.genscript.com/tools/codon-frequency-table) was applied to choose the most and least common codons in the human genome. The codons of all constructs are listed in Table S2. For analysis, the relative frequency of each codon was expressed relative to the other possible codons for the same AA.

4.3 | Cell culture and heterologous expression

Expression of the eGFP-tagged channels was performed as reported previously[18] in human embryonic kidney (HEK293) cells cultured in T25 cell culture flasks in an incubator (at 37°C and 5% CO_2) in standard cell culture medium [DMEM/F12-Medium with Glutamine (Biochrom AG, Berlin, Germany) plus 10% fetal calf serum (FCS) and 1% penicillin/streptomycin].

For imaging, cells were placed 48 h prior to examination on sterilized glass coverslips (No. 1.0, Karl Hecht GmbH & Co. KG, Sondheim, Germany) with Ø = 25 mm. The cells were incubated for ~48 h at 37°C with 5% CO_2. When reaching 60% confluence, cells were transfected with the appropriate plasmids using Lipofectamine 2000 (Thermo Fisher Scientific, Waltham, MA) according to manufacturer specifications. Unless otherwise stated, 1 µg of plasmid DNA of the corresponding construct was used.

4.4 | Confocal laser scanning microscopy

Initial microscopic screening and quantitative examination of protein sorting in cultured mammalian cell lines was performed on a confocal Leica TCS SP5 II microscope (Leica GmbH, Heidelberg, Germany). Unless stated otherwise, cells were kept with 500 µL PBS medium (8 g/L sodium chloride, 0.2 g/L potassium chloride, 1.42 g/L disodium hydrogen phosphate, 0.24 g/L potassium hydrogen phosphate; pH was adjusted with 1 M sodium hydroxide up to 7.4) on glass coverslips, clamped into a custom-made aluminum cup 16 h after transfection.

Cells were imaged with a HCX PL APO 63.0x1.20 W CORR UV lens. Dyes or fluorescent proteins were excited with an argon (488 nm), krypton (562 nm) or helium–neon laser (633 nm) and the emitted light observed at the following wavelengths: GFP: 505–535 nm, MitoTracker™ Red FM and mCherry: 590–630 nm, ER-Tracker™ Red: 600–640 nm, MitoTracker™ Deep Red: 665–690 nm.

Localization of Kesv constructs in HEK cells was assessed in a two-stage process. Targeting of eGFP-tagged Kesv proteins was first examined in HEK293 cells by examining a colocalization of the

GFP signal with that of organelle-specific markers (COXVIII::mCherry for mitochondria, HDEL::mCherry for ER) and/or organelle-specific fluorescent dyes (ER-Tracker™ Red, MitoTracker™ Deep Red, MitoTracker™ Red FM). This analysis provided three distinct sorting phenotypes in which the eGFP signal was either colocalized with (1) a mitochondria or (2) an ER-specific marker. In a third category, the GFP fluorescence was uniformly distributed throughout the cell including the nucleus (Figure 2). In some cases, we could even detect a decrease in the fluorescence signal in areas occupied by either ER or mitochondria (Figure S1A). This phenotype was classified as (3) unsorted/degraded.

To avoid an interference of Kesv sorting with the overexpression of an organelle-specific marker protein, quantification of Kesv targeting was done in the absence of organelle-specific markers. Guided by the images from the first step, we classified cells "ER-positive", when the GFP distribution showed an increased fluorescence at the perinuclear ring and in filamentous structures surrounding the nucleus. Positive targeting to "mitochondria" was identified as small structures with increased GFP signal within the cytosol. In cells in which GFP fluorescence was uniformly distributed throughout the cell including the nucleus, the Kesv protein was classified as "un-sorted".

Dye labeling was performed according to established manufacturers' protocols. The growth medium was replaced with PBS containing the organelle-specific dyes MitoTracker™ Red FM (25 nM), ER-Tracker™ Red (1 μM) or MitoTracker™ Deep Red (50 nm) (Thermo Fisher Scientific, Waltham, MA). After incubation for 5 min, cells were washed with fresh PBS buffer before imaging. As organelle-specific dyes have only a limited specificity, mitochondria and ER were in all experiments also labeled with fluorescent-specific marker proteins. The subunit VIII of human cytochrome C oxidase fused with the fluorescent protein mCherry (COXVIII::mCherry) was employed to label the inner membrane of the mitochondria. The ER retention sequence HDEL fused with fluorescent protein mCherry (HDEL::mCherry) was used to label the ER. Both plasmids were obtained from Addgene (Cambridge, MA).

To determine protein localization in the different cellular compartments, 300 cells with a fluorescent signal, collected from six distinct experiments, were imaged and analyzed manually. Image analysis was generally performed using LAS AF Lite software (Leica Microsystems GmbH, Wetzlar, Germany) or Fiji.[44]

4.5 | Data analysis

Data analysis was performed with a custom Python 3 script utilizing NumPy[45] and pandas.[46] Plots were generated with plotly (Plotly Technologies Inc. Montréal, Canada, https://plot.ly). For each codon triplet, the mean and standard deviation were calculated for parameters CUB, HyP and the product of both (CUB × HyP). The net charge was calculated as the sum of the partial charges of the three inserted AAs. Linear regression was performed on a subset of data, consisting of inserts with different AAs and a net charge of 0, using the SciPy[47] line-regress function. Randomization of CUB values of $Kesv_{+3}$ constructs and calculation of corresponding Pearson correlation coefficients for sorting to the ER as function of HyP × CUB was performed with a custom Matlab R2020b script utilizing the function perms().

The length of the ct-TMD was predicted in a three-step process. First, the AAs belonging to ct-TMD were predicted using DeepTMHMM (1.0.19).[23] Next, the structure of the full proteins was predicted using ColabFold ("AlphaFold2_mmseqs2" version 1.3.0)[48] utilizing AlphaFold2[24] and MMseqs2.[49] Finally, the distance between the initial and final alpha C-atoms in the alpha-helix was measured for each mutant using ChimeraX (1.5).[25] ChimeraX was also used to render the images. For overlays, the structures were aligned in the pore helix region (AAs 73–84).

AUTHOR CONTRIBUTIONS

Anja J. Engel: Conceptualization Investigation, Visualization, Writing Original Draft; **Steffen Paech:** Methodology, Formal analysis, Investigation, Visualization; **Markus Langhans:** Methodology; **James L. Van Etten:** Conceptualization, Writing Original Draft; **Anna Moroni:** Conceptualization, Writing Original Draft, Funding acquisition; **Gerhard Thiel:** Conceptualization, Methodology, Writing Review & Editing, Supervision, Project administration, Funding acquisition; **Oliver Rauh:** Conceptualization, Methodology, Formal analysis, Writing Review & Editing.

ACKNOWLEDGMENTS

This work was supported by the European Research Council [ERC; 2015 Advanced Grant 495 (AdG) no. 695078 noMAGIC to Anna Moroni and Gerhard Thiel), DFG priority program SPP1926 (to Gerhard Thiel) and Fondazioner Telethon grant GGP20021 MCPI (to Anna Moroni). Open Access funding enabled and organized by Projekt DEAL.

CONFLICT OF INTEREST STATEMENT

The authors declare no conflicts of interest for this article.

PEER REVIEW

The peer review history for this article is available at https://www.webofscience.com/api/gateway/wos/peer-review/10.1111/tra.12915.

DATA AVAILABILITY STATEMENT

All gene constructs generated in this study are available from O. Rauh upon reasonable request.

ORCID

Steffen Paech https://orcid.org/0000-0001-5468-8056
James L. van Etten https://orcid.org/0000-0002-5063-0049
Anna Moroni https://orcid.org/0000-0002-1860-406X
Gerhard Thiel https://orcid.org/0000-0002-2335-1351
Oliver Rauh https://orcid.org/0000-0003-1082-8656

REFERENCES

1. Koch C, Schuldiner M, Herrmann JM. ER-SURF: riding the endoplasmic reticulum surface to mitochondria. *Int J Mol Sci*. 2021;22:1-13. doi:10.3390/ijms22179655

2. Ben-Menachem R, Tal M, Shadur T, Pines O. A third of the yeast mitochondrial proteome is dual localized: a question of evolution. *Proteomics*. 2011;11:4468-4476.
3. Karniely S, Pines O. Single translation-dual destination: mechanisms of dual protein targeting in eukaryotes. *EMBO Rep*. 2005;6:420-425.
4. Grudnik P, Bange G, Sinning I. Protein targeting by the signal recognition particle. *Biol Chem*. 2009;390:775-782.
5. Borgese N, Fasana E. Targeting pathways of C-tail-anchored proteins. *Biochim Biophys Acta Biomembr*. 2011;1808:937-946.
6. Farkas Á, Bohnsack KE. Capture and delivery of tail-anchored proteins to the endoplasmic reticulum. *J Cell Biol*. 2021;220(8): e202105004. doi:10.1083/jcb.202105004
7. Gamerdinger M, Hanebuth MA, Frickey T, Deuerling E. The principle of antagonism ensures protein targeting specificity at the endoplasmic reticulum. *Science*. 2015;348:201-207.
8. Schuldiner M, Metz J, Schmid V, et al. The GET complex mediates insertion of tail-anchored proteins into the ER membrane. *Cell*. 2008; 134:634-645.
9. Aviram N, Ast T, Costa EA, et al. The SND proteins constitute an alternative targeting route to the endoplasmic reticulum. *Nature*. 2016;540:134-138.
10. Haßdenteufel S, Sicking M, Schorr S, et al. hSnd2 protein represents an alternative targeting factor to the endoplasmic reticulum in human cells. *FEBS Lett*. 2017;591:3211-3224. doi:10.1002/1873-3468.12831
11. Stojanovski D, Bohnert M, Pfanner N, van der Laan M. Mechanisms of protein sorting in mitochondria. *Cold Spring Harb Perspect Biol*. 2012;1(4):a011320. doi:10.1101/cshperspect.a011320
12. Hegde RS, Bernstein HD. The surprising complexity of signal sequences. *Trends Biochem Sci*. 2006;31:563-571.
13. Pelkmans L, Helenius A. Insider information: what viruses tell us about endocytosis. *Curr Opin Cell Biol*. 2003;15:414-422.
14. Thiel G, Baumeister D, Schroeder I, Kast SM, van Etten JL, Moroni A. Minimal art: or why small viral K^+ channels are good 641 tools for understanding basic structure and function relations. *Biochim Biophys Acta*. 2011;1808:580-588.
15. Asrani P, Seebohm G, Stoll R. Potassium viroporins as model systems for understanding eukaryotic ion channel behaviour. *Virus Res*. 2022; 320:198903. doi:10.1016/j.virusres
16. Watson HR, Wunderley L, Andreou T, Warwicker J, High S. Reorientation of the first signal-anchor sequence during potassium channel biogenesis at the Sec61 complex. *Biochem J*. 2013;456:297-309.
17. Moroni A, Viscomi C, Sangiorgio V, et al. The short N-terminus is required for functional expression of the virus encoded miniature K^+-channel Kcv. *FEBS Lett*. 2002;530:65-69.
18. Engel AJ, Winterstein LM, Kithil M, Langhans M, Moroni A, Thiel G. Light-regulated transcription of a mitochondrial-targeted K^+channel. *Cell*. 2020;9:2507.
19. Balss J, Mehmel M, Baumeister D, et al. Transmembrane domain length of viral K^+ channels is a signal for mitochondria targeting. *Proc Natl Acad Sci USA*. 2008;10:12313-12318.
20. Zhang Y, Schäffer T, Wölfle T, Fitzke E, Thiel G, Rospert S. Cotranslational intersection between the SRP and GET targeting pathways to the endoplasmic reticulum of *Saccharomyces cerevisiae*. *Mol Cell Biol*. 2016;36:2374-2383.
21. von Chappuis C, Meckel T, Moroni A, Thiel G. The sorting of a small potassium channel in mammalian cells can be shifted between mitochondria and plasma membrane. *Cell Calcium*. 2014;58:114-121.
22. Engel A, Kithil M, Langhans M, et al. Codon bias can determine sorting of a potassium channel protein. *Cells*. 2021;10:1128.
23. Hallgren J, Tsirigos KD, Pedersen MD, et al. DeepTMHMM predicts alpha and beta transmembrane proteins using deep neural networks. *bioRxiv*. 2022. doi:10.1101/2022.04.08.487609
24. Jumper J, Evans R, Pritzel A, et al. Highly accurate protein structure prediction with AlphaFold. *Nature*. 2021;596:583-589.
25. Pettersen EF, Goddard TD, Huang CC, et al. UCSF ChimeraX: structure visualization for researchers, educators, and developers. *Protein Sci*. 2021;30(1):70-82.
26. Kyte J, Doolittle RF. A simple method for displaying the hydropathic character of a protein. *J Mol Biol*. 1982;157(1):105-132.
27. Hanson G, Coller J. Codon optimality, bias and usage in translation and mRNA decay. *Nat Rev Mol Cell Biol*. 2018;19:20-30.
28. Mauro V, Chappell SA. A critical analysis of codon optimization in human therapeutics. *Trends Mol Med*. 2015;20:604-613.
29. Mateja A, Keenan RJ. A structural perspective on tail-anchored protein biogenesis by the GET pathway. *Curr Opin Struct Biol*. 2018;51:195-202.
30. Adzhubei AA, Adzhubei IA, Krasheninnikov IA, Neidle S. Non-random usage of 'degenerate' codons is related to protein three-dimensional structure. *FEBS Lett*. 1996;399:78-82.
31. Gu W, Zhou T, Ma J, Sun X, Lu Z. The relationship between synonymous codon usage and protein structure in *Escherichia coli* and Homo sapiens. *Biosystems*. 2004;73:89-97.
32. Gupta SK, Majumdar S, Bhattacharya TK, Ghosh TC. Studies on the relationships between the synonymous codon usage and protein secondary structural units. *Biochem Biophys Res Commun*. 2000;269:692-696.
33. Rosenberg AA, Marx A, Bronstein AM. Codon-specific Ramachandran plots show amino acid backbone conformation depends on identity of the translated codon. *Nat Commun*. 2022;13:2815. doi:10.1038/s41467-022-30390-9
34. Wang E, Wang J, Chen C, Xiao Y. Computational evidence that fast translation seed can increase the probability of cotranslational protein folding. *Sci Rep*. 2015;5:15316.
35. Sharma AK, Bukau B, O'Brien EP. Physical origins of codon positions that strongly influence co-translational folding: a framework for controlling nascent protein folding. *J Am Chem Soc*. 2015;138(4):1180-1195.
36. Mitra S, Ray SK, Banerjee R. Synonymous codons influencing gene expression in organisms. *Res Rep Biochem*. 2016;6:57-65.
37. Buhr F, Jha S, Thommen M, et al. Synonymous codons direct cotranslational folding toward different protein conformations. *Mol Cell*. 2016;61(3):341-351.
38. Pechmann S, Chartron JW, Frydman J. Local slowdown of translation by nonoptimal codons promotes nascent-chain recognition by SRP in vivo. *Nat Struc Mol Biol*. 2014;21:1100-1105.
39. Stein KC, Frydman J. The stop-and-go traffic regulating protein biogenesis: how translation kinetics controls proteostasis. *J Biol Chem*. 2019;294:2076-2084.
40. Yu CH, Dang Y, Zhou Z, et al. Codon usage influences the local rate of translation elongation to regulate co-translational protein folding. *Mol Cell*. 2015;59(5):744-754.
41. Zhou M, Guo J, Cha J, et al. Non-optimal codon usage affects expression, structure and function of clock protein FRQ. *Nature*. 2013;495:111-115.
42. Dao Duc K, Song YS. The impact of ribosomal interference, codon usage, and exit tunnel interactions on translation elongation rate variation. *PLoS Genet*. 2018;14:e1007166. doi:10.1371/journal.pgen.1007166
43. DeCero SA 2nd, Winslow CH, Coburn J. Method to overcome inefficiencies in site-directed mutagenesis of a/T-rich DNA. *J Biomol Tech*. 2020;31(3):94-99.
44. Schindelin J, Arganda-Carreras I, Frise E, et al. Fiji: an open-source platform for biological-image analysis. *Nat Methods*. 2012;9:676-682.
45. Harris CR, Millman KJ, van der Walt SJ, et al. Array programming with NumPy. *Nature*. 2020;585:357-362.
46. Pandas Development Team. pandas-dev/pandas: Pandas (v1.5.3). *Zenodo*. 2023. doi:10.5281/zenodo.7549438
47. Virtanen P, Gommers R, Oliphant TE, et al. SciPy 1.0: fundamental algorithms for scientific computing in python. *Nat Methods*. 2020;17: 261-272.
48. Mirdita M, Schütze K, Moriwaki Y, Heo L, Ovchinnikov S, Steinegger M. ColabFold: making protein folding accessible to all. *Nat Methods*. 2022;19:679-682. doi:10.1038/s41592-022-01488-1

49. Evans R, O'Neill M, Pritzel A, et al. Protein complex prediction with AlphaFold-multimer. bioRxiv 2021.10.04.463034. 2022. doi:10.1101/2021.10.04.463034

SUPPORTING INFORMATION

Additional supporting information can be found online in the Supporting Information section at the end of this article.

How to cite this article: Engel AJ, Paech S, Langhans M, et al. Combination of hydrophobicity and codon usage bias determines sorting of model K^+ channel protein to either mitochondria or endoplasmic reticulum. *Traffic*. 2023;24(11):533-545. doi:10.1111/tra.12915